

ApoFnr Binds as a Monomer to Promoters Regulating the Expression of Enterotoxin Genes of *Bacillus cereus*[†]

Julia Esbelin,¹ Yves Jouanneau,² Jean Armengaud,³ and Catherine Duport^{1*}

Université d'Avignon, UMR A408, Sécurité et Qualité des Produits d'Origine Végétale, and INRA, Avignon, F-84914, France¹; Laboratoire de Chimie et Biologie des Métaux, UMR 5249, CEA, DSV, iRTSV, CEA-Grenoble Cedex 09, F-38054, France²; and Laboratoire de Biochimie des Systèmes Perturbés, CEA-Marcoule, SBTN, BP17171, Bagnols-sur-Cèze Cedex, F-30207, France³

Received 7 March 2008/Accepted 11 April 2008

Bacillus cereus Fnr is a member of the Crp/Fnr (cyclic AMP-binding protein/fumarate nitrate reduction regulatory protein) family of helix-turn-helix transcriptional regulators. It is essential for the expression of *hbl* and *nhe* enterotoxin genes independently of the oxygen tension in the environment. We studied aerobic Fnr binding to target sites in promoters regulating the expression of enterotoxin genes. *B. cereus* Fnr was overexpressed and purified as either a C-terminal His-tagged (Fnr_{His}) fusion protein or an N-terminal fusion protein tagged with the Strep-tag (IBA BioTAGnology) (Strep⁺Fnr). Both recombinant Fnr proteins were produced as apoforms (clusterless) and occurred as mixtures of monomers and oligomers in solution. However, apoFnr_{His} was mainly monomeric, while apoStrep⁺Fnr was mainly oligomeric, suggesting that the His-tagged C-terminal extremity may interfere with oligomerization. The oligomeric state of apoStrep⁺Fnr was dithiothreitol sensitive, underlining the importance of a disulfide bridge for apoFnr oligomerization. Electrophoretic mobility shift assays showed that monomeric apoFnr, but not oligomeric apoFnr, bound to specific sequences located in the promoter regions of the enterotoxin regulators *fnr*, *resDE*, and *plcR* and the structural genes *hbl* and *nhe*. The question of whether apoFnr binding is regulated in vivo by redox-dependent oligomerization is discussed.

The facultative anaerobic, spore-forming *Bacillus cereus* has gained notoriety as an opportunistic human pathogen that can cause a wide range of diseases from periodontitis and endophthalmitis to meningitis in immunocompromised patients. However, most of the reported illnesses involving *B. cereus* are food-borne intoxications, classified as emetic and diarrheal syndromes (17, 30). Diarrheal syndrome may result from the production in the human host's small intestine of various extracellular factors including hemolysin BL (Hbl), nonhemolytic enterotoxin (Nhe), and cytotoxin CytK (17, 26). The genes encoding these potential virulence factors belong to the PlcR regulon (1, 7, 20, 31).

B. cereus will grow efficiently by anaerobic glucose fermentation in amino acid-rich media supplemented with glucose as the major source of carbon and energy (3, 21, 29, 33, 34). The ability of *B. cereus* to grow well under these conditions is controlled by both the two-component system ResDE (4) and the redox regulator Fnr (33, 34). Unlike ResDE, *B. cereus* Fnr has been shown to be essential for fermentative growth and for enterotoxin synthesis under both anaerobiosis and aerobiosis (33, 34). Fnr protein is a member of the large Crp/Fnr (cyclic AMP-binding protein/fumarate nitrate reduction regulatory protein) superfamily of transcription factors that coordinate physiological changes in response to a variety of metabolic and environmental stimuli (16). Members of the family are pre-

dicted to be structurally related to the catabolite gene activator protein of *Escherichia coli*, Crp (also known as the cyclic AMP receptor protein) (10). Like all the members of the Crp/Fnr family, *B. cereus* Fnr contains an N-terminal region made up of antiparallel β -strands able to accommodate a nucleotide, and a C-terminal helix-turn-helix structural motif. In addition, it contains a C-terminal extension with four cysteine residues considered, in *Bacillus subtilis*, to coordinate a $[4\text{Fe-4S}]^{+2}$ center that serves as a redox sensor (27). The *B. subtilis* Fnr forms a stable dimer that is independent of both the oxygen tension in the environment and FeS cluster formation. However, the presence of an intact $[4\text{Fe-4S}]^{+2}$ cluster is required for it to bind to a specific DNA-binding site and for subsequent transcriptional activation (27).

Structurally, the predicted Fnr of *B. cereus* resembles the *B. subtilis* Fnr (27). Therefore, the FeS cluster could also be a key component required for the DNA-binding activity of *B. cereus* Fnr under anaerobiosis. However, our previous results suggested that unlike *B. subtilis* Fnr, *B. cereus* Fnr may also exist in an active state under aerobiosis and thus conserve some site-specific DNA-binding properties. To address this specificity further and elucidate the mechanism by which Fnr regulates enterotoxin gene expression in aerobically growing *B. cereus* cells, we characterized the DNA-binding activities of purified aerobic Fnr. To this end, we overproduced full-length Fnr in *Escherichia coli* with two different tags. We showed that both recombinant Fnr proteins were produced in apo forms (devoid of FeS cluster) under oxic conditions. Recombinant Fnr containing a C-terminal polyhistidine-tagged sequence was shown to be mainly monomeric in solution, while N-terminally Strep-tagged Fnr occurred mainly as oligomers. Only the monomeric forms of both recombinant apoFnr proteins were found to bind

* Corresponding author. Mailing address: UMR A408, INRA, Site Agroparc, 84914 Avignon Cedex 9, France. Phone: 33 4 32 72 25 07. Fax: 33 4 32 72 24 92. E-mail: catherine.duport@univ-avignon.fr.

[†] Supplemental material for this article may be found at <http://jb.asm.org/>.

[‡] Published ahead of print on 18 April 2008.

to the promoter regions of *fnr* itself, the pleiotropic regulator genes *resDE* and *plcR*, and the structural enterotoxin genes *hbl* and *nhe*. Finally, our results pointed to some new unusual properties of Fnr that may have physiological relevance in the redox regulation of enterotoxin expression, enterotoxin expression being both directly and indirectly (via ResD and PlcR) regulated by apoFnr under aerobiosis.

MATERIALS AND METHODS

Bacterial strains and growth conditions. *Escherichia coli* strain TOP 10 (Invitrogen) [F^- *mcrA* Δ (*mrr-hsdRMS-mcrBC*) ϕ 80lacZ Δ M15 Δ lacX74 *deoR* *recA1* *araD139*(*ara-leu*)7697 *galU* *galK* *rpsL* (Str^r) *endA1* *nupG*] was used as the general cloning host, and strain BL21 CodonPlus(DE3)-RIL (Stratagene) [F^- *ompT* *hsdS*(r_B^- m_B^-) *dcm*⁺ Tet^r *gal* λ (DE3) *endA* Hte [*argU* *ileY* *leuW* Cam^r]] was used to overexpress *fnr*. Both *E. coli* strains were routinely grown in Luria broth with vigorous agitation at 37°C. The wild-type *B. cereus* F4430/73 (32) and *fnr* mutant (34) were grown as previously described.

General molecular methods. Restriction endonuclease and T4 DNA ligase were obtained from Promega and used in accordance with the manufacturer's instructions. Genomic DNA of *B. cereus* was purified by the method of Guinbreiere and Nguyen-The (11). Plasmid DNA was purified using anion-exchange columns (Promega). PCR amplification of DNA was carried out with *Taq* polymerase using the manufacturer's specifications (Roche Molecular Biochemicals) for reaction conditions. The 5' end of the *resDE* mRNA was mapped from a 5' rapid amplification of cDNA ends (5' RACE) PCR product obtained with the 3'/5' RACE kit (Roche Molecular Biochemicals). For this purpose, we used total RNA extracted from *B. cereus* F4430/73 cells harvested at μ_{max} , i.e., the maximal expression of the *resDE* operon. Briefly, the first-strand cDNA was synthesized from total RNA with *fnr*-specific primer SP1 (5'-GCCTGGTAAAGATGGCA TTG-3'), avian myeloblastosis virus reverse transcriptase, and the deoxynucleotide mixture of the 3'/5' RACE kit as recommended by the manufacturer. After purification and dA tailing of the cDNA, a PCR with the dT anchor oligonucleotide primer and the specific *fnr* SP2 primer (5'-GATGATGAGGATCGTATT VGTGCG-3'), followed by a nested PCR with SP3 primer (5'-GAGAGTGCAG AGCGGGTAGAG-3'), yielded a PCR product of 190 bp, as revealed by 2% agarose gel electrophoresis. This PCR product was purified and sequenced.

Cloning and overexpression of recombinant Fnr. The coding sequence for *B. cereus* *fnr* was PCR amplified from *B. cereus* F4430/73 genomic DNA using either primers PET101F (5'-CACGTGGCAAACAGTATGACATTATCT-3') and PET101R (5'-ATCAATGCTACAAA CAGAAGC-3') or primers PET52F (5'-CCCGGATGACATTATCTCAAGATTAAAAAGAA-3'; SmaI restriction site in bold type) and PET52R (5'-GAGCTCCTAATCAATGCTACAAACAG AAGCA-3'; SacI restriction site in bold type). The amplicons were cloned as a blunt-end PCR product into pET101/D-TOPO (Invitrogen) and as a SmaI-SacI fragment into the corresponding sites of pET-52b(+) (Novagen), yielding pET101/*fnr* and pET52/*fnr*, respectively. *B. cereus* Fnr was produced as a C-terminal fusion with a His tag (Fnr_{His}) using pET101/*fnr* and as an N-terminal fusion with a Strep-tag (IBA BioTAGnology) (Strep_{His}Fnr) using pET52/*fnr* in *E. coli* BL21 CodonPlus(DE3)-RIL (Stratagene). Recombinant cells were grown at 37°C in Luria broth with 100 μ g ml⁻¹ ampicillin. When the optical density at 600 nm reached ~1.0, protein production was triggered by adding isopropyl- β -D-thiogalactopyranoside (IPTG) with a final concentration of 0.2 mM (pET101/*fnr*) or 0.4 mM (pET52/*fnr*). Cells were grown for 16 h at 20°C.

Purification of Fnr_{His}. Cells from a 4.8-liter culture were harvested by centrifugation (10,000 \times g, 15 min), resuspended in buffer A (50 mM sodium phosphate buffer [pH 7.0], 300 mM NaCl), and incubated with 0.5 mg/ml lysozyme for 30 min under gentle agitation. Cells were lysed by sonication for 3 min at 80% of maximum amplitude using a Vibra cell ultrasonifier (Fisher Bioblock Scientific). Cell debris was removed by centrifugation at 20,000 \times g for 20 min. The supernatant was run through a 5-ml Co²⁺ immobilized metal ion affinity chromatographic column (Clontech) equilibrated with buffer A. The column was washed with 50 ml of buffer A and then with 25 ml of buffer A containing 10 mM imidazole, and the protein was eluted with 5 ml of buffer A containing 150 mM imidazole. The eluted fraction was desalted on a Sephadex G25 column (Amersham Pharmacia Biotech) and concentrated using Nanosep 30-kDa molecular-mass-cutoff devices (Omega disc membrane; Pall Filtron). Concentrated samples were run through a 104-ml Superdex SD200 column (Amersham Biosciences) equilibrated with buffer B (100 mM Tris-HCl [pH 8], 150 mM NaCl, 1 mM dithiothreitol [DTT]). Protein was stored as pellets in liquid nitrogen.

Purification of Strep_{His}Fnr. Cells from a 6-liter culture were harvested by centrifugation at 10,000 \times g for 15 min, resuspended in 120 ml of buffer C (25 mM Tris-HCl [pH 8], 1 mM DTT), and incubated with 0.2 mg \cdot ml⁻¹ of lysozyme and 0.5 mM EDTA for 10 min at 30°C. Cells were lysed by sonication as described above for the purification of Fnr_{His}. Cell debris was removed by centrifugation at 43,000 \times g for 1 h, and the resulting supernatant was run through a 30-ml DEAE-cellulose column (DE52; Whatman) equilibrated with buffer C. The column was then washed with the same buffer. Nonretained fractions were adjusted to pH 7 with 1 M KH₂PO₄ and run through a 30-ml hydroxyapatite agarose column (HA Ultrogel; Pall Corporation) equilibrated with buffer D (50 mM KH₂PO₄ [pH 7], 1 mM DTT). The column was developed with a linear gradient from 50 to 200 mM KH₂PO₄ at a flow rate of 2 ml/min. Fractions containing recombinant Fnr were pooled and concentrated to 48 mg \cdot ml⁻¹ by ultrafiltration through an Omega disc membrane (30-kDa cutoff; diameter, 43 mm; Pall Filtron). A polishing step was then carried out with gel filtration on a 104-ml Superdex SD200 column (Amersham Biosciences) equilibrated with buffer D containing 150 mM NaCl. The purified protein was stored as pellets in liquid nitrogen.

Protein biochemical analyses. Protein concentrations were determined by either a bicinchoninic acid assay according to the manufacturer's instructions (Interchim) or a biuret method insensitive to thiols (22). Bovine serum albumin was used as a standard. Overproduction of Fnr in induced cultures and its purification were monitored by sodium dodecyl sulfate-polyacrylamide gel electrophoresis (SDS-PAGE). The Laemmli method was used for SDS-PAGE (18). Proteins were stained with Coomassie brilliant blue. The reducing agent β -mercaptoethanol was omitted to analyze the disulfide form of apoFnr. The molecular mass of apoFnr was accurately measured with an Esquire 3000plus ion trap mass spectrometer equipped with a nanoelectrospray on-line ion source (Bruker Daltonics) essentially as described previously (6). Before mass measurement, purified apoFnr was desalted with a ZipTipC18 (Millipore) and diluted in 50% acetonitrile-1% formic acid (vol/vol).

DLS. The quaternary structure of purified apoFnr in solution was measured by dynamic light scattering (DLS). Samples were centrifuged and run through a 24-ml Superdex 200 column (HR10/30) equilibrated and run at a flow rate of 0.5 ml/min with 50 mM Tris-HCl (pH 8.3) containing 120 mM NaCl and 0.05% Na₂S, filtered at 0.1 μ m. The column was operated with an Agilent 1100 series reverse-phase high-performance liquid chromatography system equipped with a G1322A degasser, G1311A quaternary pump, and G1313A autosampler. The elution profile was monitored with a G1315B diode array detector (Agilent), a miniDawn Tristar multiangle laser static light scattering detector (three angles, 45°, 90°, and 135°) coupled to a DynaPro Titan light scattering instrument (Wyatt Technology) placed at 90° and an Optilab rEX differential refractometer (Wyatt Technology). The 90° multiangle light scattering detector was calibrated with pure toluene, and bovine serum albumin was then used to normalize the other detector (45° and 135°) in the corresponding buffer.

Chemical cross-linking of Fnr_{His}. Fnr_{His} in 10 mM 3-(*N*-morpholino)propane-sulfonic acid (MOPS) buffer (pH 7.75) was treated with protein cross-linking agents, *N*-hydroxysulfosuccinimide (5 mM) and 1-ethyl-3-[3-dimethylaminopropyl]carbodiimide hydrochloride (EDC) (12.5 mM). The reaction mixture contained protein at a concentration of 5 μ M in a total reaction mixture volume of 20 μ l. The reaction was allowed to proceed for 30 min at room temperature and stopped by adding 25 mM β -mercaptoethanol. The products were analyzed by 12% nondenaturing SDS-PAGE and detected by Western blotting using an anti-His antibody.

ApoFnr antiserum preparation. Polyclonal antibodies against apoFnr were generated in-house. Rabbits were immunized with a total of 2 mg of purified Fnr_{His}, administered in four equal doses over a 90-day period, and bled on day 120. Antisera specificities were checked by Western blotting.

Western blot analysis. *B. cereus* protein extracts were prepared as follows: cells were harvested by centrifugation, resuspended in buffer containing 8 M urea, 4% (wt/vol) CHAPS ([3-[(3-cholamidopropyl)-dimethylammonio]propanesulfonate]), and mechanically disrupted using a FastPrep instrument (FP120; Bio101, Thermo Electron Corporation). Cell debris was removed by centrifugation (3,500 \times g, 10 min, 4°C). Proteins were then filtered and resolved by SDS-PAGE under nonreducing conditions (18). Resolved proteins were transferred to nitrocellulose membranes (Amersham Bioscience) in a Bio-Rad liquid/liquid transfer unit. As appropriate, apoFnr was detected with either anti-His antibodies (Fnr_{His}) or anti-Strep antibodies (Strep_{His}Fnr) or with a 1:2,000 dilution of polyclonal rabbit serum. The blotted membranes were developed with a 1:2,000 dilution of peroxidase-conjugated goat anti-rabbit immunoglobulin G (Sigma) and an enhanced chemiluminescence substrate (Immobilon Western; Millipore).

EMSA. The 5' untranslated regions (5' UTRs) of *fnr*, *resDE*, *plcR*, *hbl*, and *nhe* were PCR amplified with the following primer pairs: FnrF (5'-CGAACAATTC

AGCAGGCATA-3') and FnrR (5'-AATGTCATACTGTTTGCAC-3'), ResDF (5'-TGGGATCCCAAAGAGGTTTG-3') and ResDR (5'-CGATCCTCATC ATCTACAAT-3'), PlcRF (5'-TATGTTTGTGCAAGGCGAAC-3') and PlcRR (5'-CCTAATTTTCTGCGTGCAT-3'), Hbl1F (5'-GGTAAGCAAGTGGGT GAAGC-3') and Hbl1R (5'-AATCGCAAATGCAGAGCACAA-3'), Hbl2F (5'-TTAACTTAATTCATATAACTT-3') and Hbl2R (5'-TACGCATTAATAA TTTAAT-3'), and NheF (5'-TGTTATTACGACAGTTCCAT-3') and NheR (5'-CTGTAACCAATAACCCTGTG-3'). The forward primers were 5' end labeled with T4 polynucleotide kinase (Promega) and [γ - 32 P]ATP (Amersham Biosciences). The 5'- 32 P-labeled amplicons were purified using High Pure PCR product purification columns (Roche). Electrophoretic mobility shift assays (EMSAs) were performed by incubating labeled DNA fragments (1,000 cpm per reaction mixture) with the specified amount of purified Fnr in 50 mM Tris-HCl (pH 7.5) buffer containing 50 mM KCl, 0.1 mM EDTA, 10% glycerol, 4 mM DTT, 4 mM MgCl₂, 0.5 μ g of bovine serum albumin, and 1 μ g of poly(dI-dC)/ml in a final volume of 10 μ l. Binding reaction mixtures were incubated for 30 min at 37°C and then loaded onto a 4% or 6% nondenaturing polyacrylamide gel run with Tris-borate-EDTA buffer at 4°C and 200 V. Labeled products were quantified using a Molecular Dynamics PhosphorImager.

RESULTS

Overexpression and purification of two recombinant Fnr proteins. From the sequence alignment of 13 *B. cereus* Fnr homologues (see Fig. S1 in the supplemental material), two possible alternative translation initiation starts could be identified for *B. cereus* F4430/73: GTG as previously defined (34) or ATG 12 nucleotides further on. Taking into account this information, two procedures were developed for the aerobic production of *B. cereus* F4430/73 Fnr in *E. coli* cells: (i) expression of a His-tagged fusion protein from pET101/D-TOPO to release a Fnr variant (Fnr_{His}) that begins with the valine encoded by the predicted start codon of *B. cereus* (34) and contains 30 additional amino acids at the C-terminal end, and (ii) expression of a protein from pET-52b(+) fused to *Strep*-tag (IBA BioTAGnology) to release an Fnr variant (Fnr_{Strep}) that contains 22 additional amino acids at the N-terminal end. In the latter variant, the first amino acid of the native Fnr is the methionine located four amino acids after the valine encoded by the predicted start codon (see Fig. S1 in the supplemental material). The Fnr_{His} protein was purified using cobalt affinity chromatography. Because preliminary tests indicated that Fnr_{Strep} bound very weakly to *Strep*-Tactin Sepharose (IBA BioTAGnology), the tagged protein was purified by means of three successive chromatography runs not based on the tag affinity. On SDS-polyacrylamide gels, purified Fnr_{His} (29 kDa) and Fnr_{Strep} (28 kDa) exhibited the expected molecular masses (see Fig. S2 in the supplemental material). The exact average molecular mass of Fnr_{Strep} determined by mass spectrometry was $27,913 \pm 2$ Da. This value corresponds almost perfectly (75-ppm deviation) to the expected polypeptide sequence, except that the initial formyl-methionine is cleaved (theoretical value of 27,911 Da). This maturation probably also occurs with the Fnr_{His} protein.

UV-visible absorption spectrum of both aerobic recombinant forms of Fnr showed a single peak at 280 nm (data not shown), suggesting that there is no absorbing prosthetic group (14). This indicates that both recombinant Fnr forms were purified as apoproteins under aerobiosis.

Oligomeric state of both recombinant apoFnr proteins. DLS was used to examine the oligomeric state of the two recombinant forms of apoFnr. DLS reveals the homogeneity and oligomeric state of proteins when resolved by gel filtration based on

the scattering of visible light by particles (5). The oligomerization states of Fnr_{His} and Fnr_{Strep} were analyzed using a DynaPro Titan DLS instrument and attendant software ASTRA. Figure 1 shows the elution profiles obtained for both proteins and the molecular mass estimates derived from the light scattering signal. Besides a peak of aggregates at 16 min, Fnr_{His} was resolved into four elution peaks at 22.0 (A1), 26.6 (A2), 28.8 (A3), and 30.7 (A4) min elution time as detected on the UV trace (Fig. 1A). The molar mass across peak A1 could not be determined because of a polydisperse distribution (the molecular mass varied from 170 to 400 kDa). This strongly suggests that this peak contained aggregates that interacted with the column, but their proportion was low, as the DLS signal was very weak. In contrast, the distribution of molar masses across peaks A2, A3, and A4 was constant, indicating a monodisperse distribution (i.e., a homogeneous molecule) for each peak with molecular masses of 98 (A2), 60 (A3), and 30 (A4) kDa ($\pm 3\%$). This indicates that Fnr_{His} occurs mainly as a mixture of trimers, dimers, and monomers in solution. Considering the relative mass ratio that can be estimated from the UV trace, the predominant form was the monomer (70%). The light scattering trace obtained with Fnr_{Strep} showed the presence of aggregates (peak B1) and three peaks with molecular masses of 157 (B2), 106 (B3), and 54 (B4) kDa ($\pm 3\%$) (Fig. 1B). These peaks unambiguously correspond to the hexameric, tetrameric, and dimeric forms of Fnr_{Strep}, respectively. In this case, the dimeric form (33%) formed the largest population. The same DLS experiment was repeated in reducing conditions with 10 mM DTT in the elution buffer. Complete disappearance of the hexameric form and almost complete disappearance of the tetrameric form (C1) were observed (Fig. 1C). The dimeric form (C2) was thus predominant (89%). Hence, the addition of reductant affected the oligomerization state of Fnr_{Strep} in solution. Intermolecular disulfide bridges are involved in the formation of the highest oligomeric forms. In addition, the absence of monomers in reducing conditions suggests that the dimers observed were either noncovalently linked structures or DTT-resistant, covalently linked structures.

When purified Fnr_{Strep} underwent SDS-PAGE under non-reducing conditions (no DTT or β -mercaptoethanol), a multiple-band pattern was observed, revealing the presence of a mixed population of monomeric, dimeric, and higher oligomeric forms in relative ratios compatible with those found in a DLS experiment (Fig. 2A). Under reducing conditions (with DTT), the two major species were the monomeric and dimeric forms. Increasing the concentration of DTT from 10 mM to 200 mM caused the total reduction of dimeric species to monomeric forms. These data indicate that most of the protein was reticulated through disulfide bridges, but a significant amount of dimeric Fnr_{Strep} could either not be completely reduced by DTT or remained particularly stable in the electrophoresis conditions used. In contrast, only a very small fraction of Fnr_{His} was found to remain dimeric after 10 mM DTT treatment (Fig. 2B). This suggests that the oligomeric Fnr_{His} population detected by DLS contained mainly noncovalently linked structures. To investigate the ability of monomeric Fnr_{His} to form covalently linked structures, a fraction of the purified protein was treated with either the chemical cross-linker EDC or with the divalent thiol-reactive agent diamide.

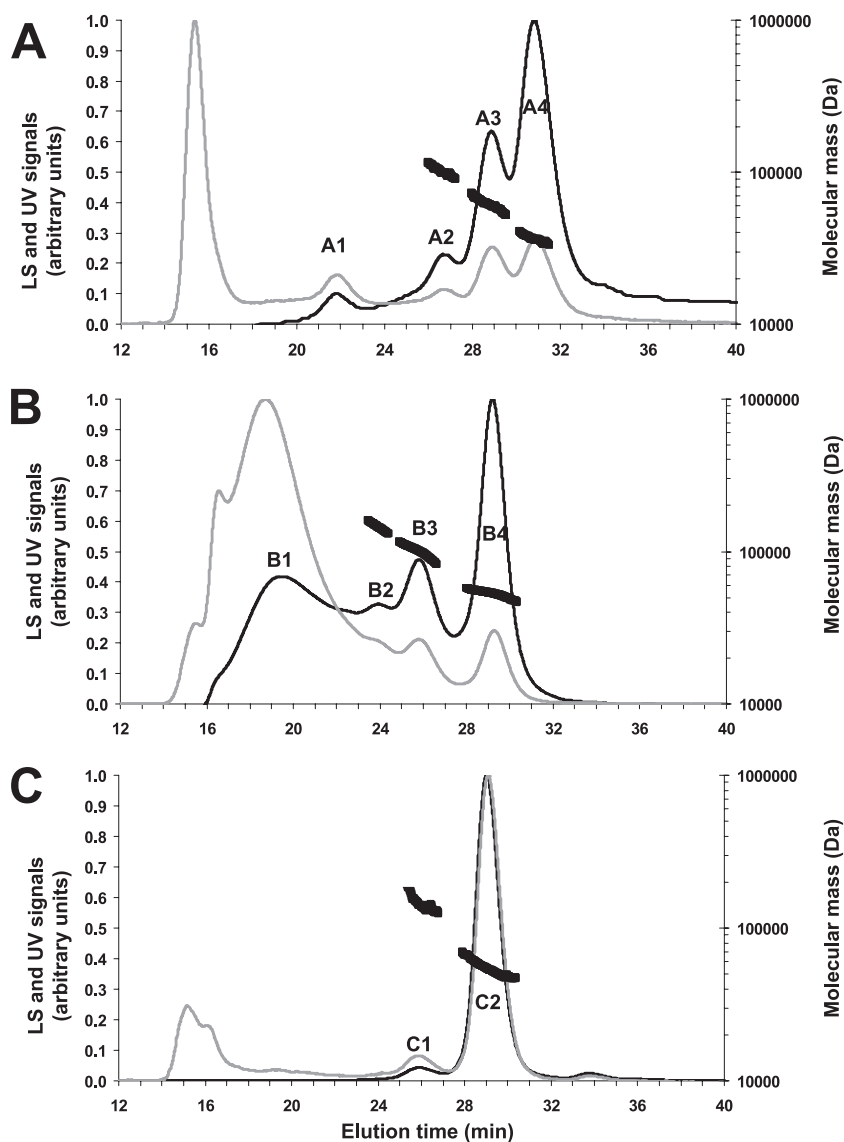


FIG. 1. Gel filtration and DLS chromatograms of purified Fnr proteins. Fnr_{His} (A), Strep⁺Fnr (B) and reduced Strep⁺Fnr (C) were injected (~300 μ g in 100 μ l) into a Superdex 200 column (HR 10/30) with 50 mM Tris-HCl (pH 8.3)-120 mM NaCl as the eluant at a flow rate of 0.5 ml/min. DTT (10 mM) was added to the elution buffer to determine the oligomeric state of reduced Strep⁺Fnr in panel C. The black and gray lines correspond to the light scattering (LS) signal and the UV signal recorded at 280 nm, respectively. These signals were normalized as a ratio from 0.0 to 1.0 for comparison (left y axis). The molecular mass estimates of the major peaks are also indicated by thick black broken lines (right y axis).

The first cross-linker modifies an ionic interaction into a covalent link, while the latter mimics disulfide bridge formation. Figure 2 shows the reaction products analyzed by SDS-PAGE. The formation of oligomers from monomers could be evidenced using both EDC (Fig. 2C) and diamide (Fig. 2D). Homodimers and homotrimers were the major products. As expected when using cross-linkers, these entities migrated at relative molecular weights slightly lower than the exact weights because of their more rigid structures. Surprisingly, the band corresponding to apoFnr monomer appeared as a discrete doublet after treatment with diamide, reflecting a possible induced conformational change trapped by intrapolypeptide cross-links (Fig. 2D). In conclusion, Fnr_{His} monomers were able to self-associate and form higher-order covalently linked

structures in the presence of cross-linkers. This suggests that unlike Strep⁺Fnr, Fnr_{His} does not tend to form covalently linked homodimers or, more specifically, intermolecular disulfide bridges.

Detection of endogenous apoFnr in *B. cereus* F4430/73 cells.

To determine whether the formation of disulfide-linked homodimers might be of physiological relevance, we tested the presence of various forms of endogenous apoFnr in aerobically grown *B. cereus* cells (4). Figure 3 shows the Western blot detection performed with apoFnr antiserum following SDS-PAGE under nonreducing conditions. The antiserum reacted with two bands of the sizes expected for the monomeric (~30-kDa) and dimeric forms (~60-kDa) of apoFnr in wild-type cells, but not in *fnr* mutant cells. Two other protein bands of 40

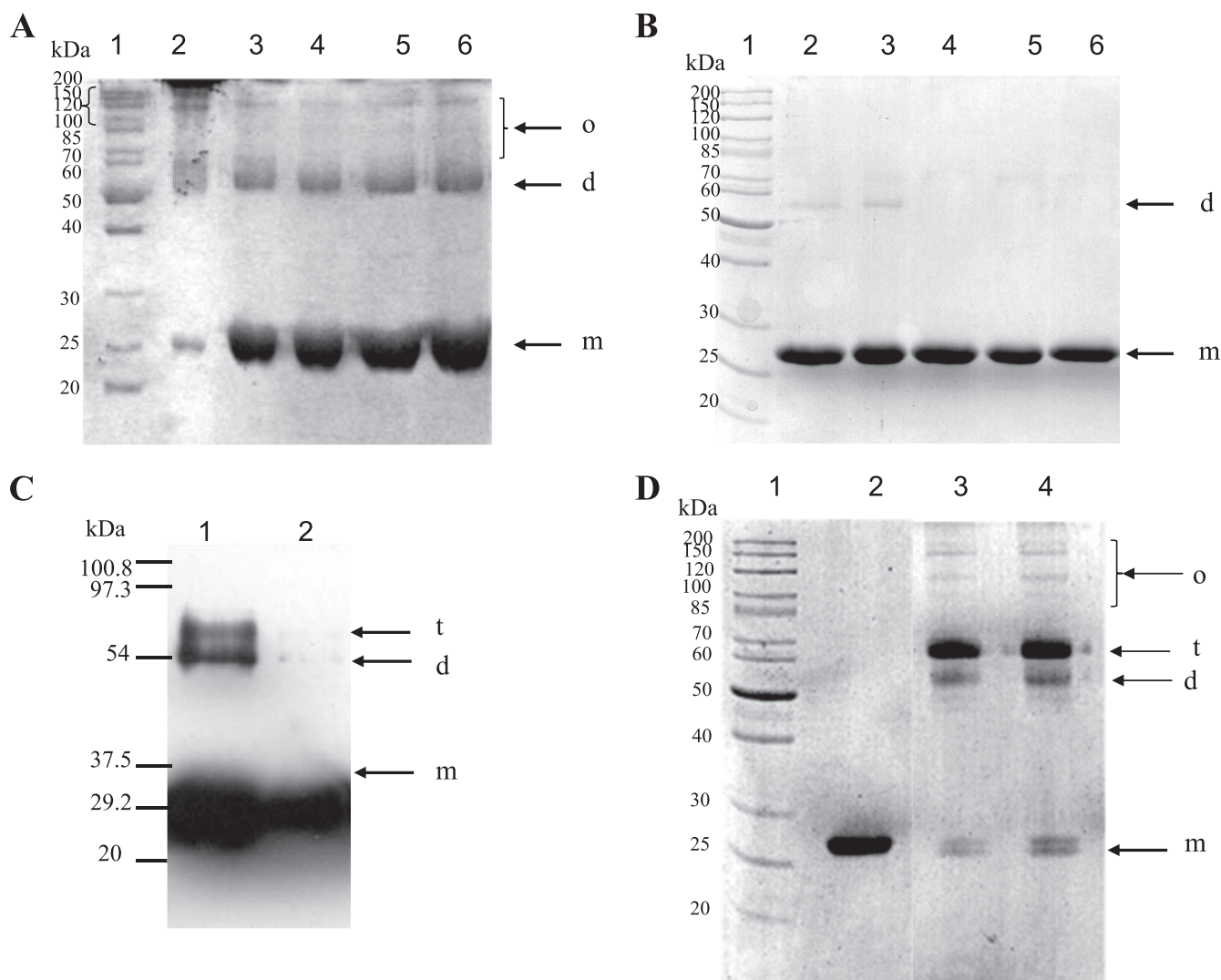


FIG. 2. SDS-PAGE analysis of the oligomeric nature of *Strep-Fnr* and *Fnr_{His}*. (A and B) Effect of DTT on *Strep-Fnr* (A) and *Fnr_{His}* (B) oligomerization. Purified proteins were incubated with 0, 10, 50, 100, or 200 mM DTT (lanes 2 to 6, respectively). Recombinant proteins were then subjected to nonreducing SDS-PAGE. The arrows show the positions of monomers (m), dimers (d), and higher oligomers (o). Lane 1 contains molecular mass standard proteins. (C) SDS-PAGE profile of *Fnr_{His}* cross-linked with EDC. *Fnr_{His}* (5 μ M) was cross-linked with EDC. Products were visualized by immunoblotting with anti-His antibody. Lane 1, cross-linked *Fnr_{His}*; lane 2, untreated *Fnr_{His}*. (D) Nondenaturing SDS-PAGE profile of *Fnr_{His}* cross-linked with diamide. Lane 1, molecular mass standard proteins; lane 2, untreated *Fnr_{His}*; lanes 3 and 4, disulfide-linked *Fnr_{His}* with 1 mM and 10 mM diamide, respectively. The arrows show the positions of monomers (m), dimers (d), trimers (t), and higher oligomers (o).

and 80 kDa cross-reacted with apoFnr antiserum in wild-type cells (Fig. 3, lane 3). As these bands were also observed in the *fnr* mutant cells (Fig. 3, lane 2), they were not related to Fnr. Finally, these results indicated that the apoFnr antiserum can be used efficiently for the detection of endogenous apoFnr in *B. cereus* F4430/73 cells and, more importantly, that some dimeric apoFnr could be disulfide linked in *B. cereus*.

Binding of apoFnr to the 5'UTRs of *fnr*, *resDE*, *plcR*, *hbl*, and *nhe*. The amino acid residues forming the REX₃R motif within the helix-turn-helix DNA-binding domain of Crp regulatory proteins are strictly conserved in the potential DNA-binding domain of *B. cereus* F4430/73 Fnr as in its homologues found in strains belonging to the *B. cereus* group (12). Accordingly, Fnr of *B. cereus* F4430/73 was assumed to bind to DNA motifs

similar to the TGTGAN₆TCACA consensus sequence defined in previous work (2, 16). Using the Virtual tool of the Prodigic database and the corresponding *E. coli* Crp position weight matrix, we scanned the 5'UTRs of regulatory and structural genes of *B. cereus* F4430/73 enterotoxins. Figure 4A shows the locations of predicted Fnr-binding boxes for *fnr*, *resDE*, *plcR*, *nhe*, *hbl1*, and *hbl2* promoters and their positions relative to the transcriptional start point of each gene/operon. Except for *resDE* (Fig. 4B), the transcriptional start sites were identified in previous studies (1, 4). Three putative Fnr-binding sites were found in the 5'UTRs of the enterotoxin gene regulators *fnr*, *resDE*, and *plcR*. Eight potential Fnr-binding sites were found in the *nhe* promoter region: four were located upstream of the transcriptional start site and four were downstream. The *hbl*

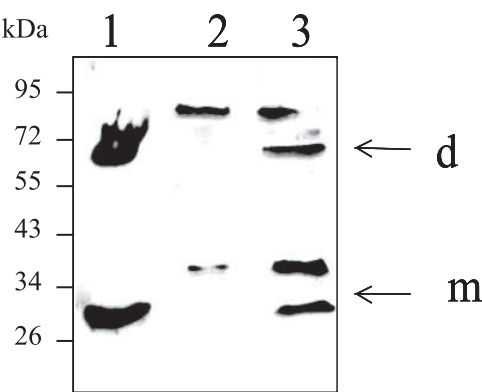


FIG. 3. Western blot detection of endogenous Fnr species from *B. cereus* cells. Lysates of wild-type *B. cereus* F4430/73 and *fnr* mutant were probed with polyclonal Fnr antiserum. Both strains were grown in regulated batch culture (pH 7.2) under aerobiosis (4). Proteins were separated by nonreducing SDS-PAGE. Lane 1, *Strep*⁺Fnr purified from *E. coli*; lane 2, *fnr* mutant; lane 3, wild-type strain. The putative identities shown on the right were determined for the wild-type strain on the basis of results obtained with both recombinant Fnr and *fnr* mutant strains. The arrows show the positions of monomer (m) and dimer (d) forms. The positions and masses (in kilodaltons) of molecular mass markers are given to the left of the gel.

promoter region contained 11 potential Fnr-binding sites, 4 located upstream of the +1 site and 7 downstream.

To test whether apoFnr bound to the Fnr boxes predicted from the nucleotide sequence analysis, EMSAs were performed with both *Strep*⁺Fnr and Fnr_{His} and DNA fragments containing 5'UTRs of *fnr*, *resDE*, *plcR*, *hbl*, and *nhe*. In view of its size (1,157 bp), the 5'UTR of *hbl* was first divided into two overlapping fragments of 636 bp (*hblI*) and 610 bp (*hbl2*) as defined in Fig. 4A. Figure 5 shows the EMSA results for the six fragments. Fnr_{His} bound to all the regions tested, while no DNA-binding activity could be detected with *Strep*⁺Fnr. The specificity of the binding was evidenced from the disappearance of complexes in competition assays using 50-fold excess of homologous unlabeled promoter regions and by the absence of any competition when an unlabeled heterologous DNA was used (data not shown). EMSAs with the negative control (Fig. 5G) showed that a shift above 6 μM apoFnr should be considered the result of nonspecific binding. In addition, the behavior of apoFnr differed markedly in the gel-shift titration assay depending on the promoter regions. ApoFnr bound to *fnr* and *resDE* promoter regions in an ordered fashion giving two retarded species (complex I and II) below 6 μM. In contrast, an increasing amount of apoFnr resulted in a gradual decrease in the mobility of the protein-DNA complexes for *plcR*, *hbl*, and *nhe* promoter regions, which appeared to be stabilized at higher protein concentrations. This suggests that,

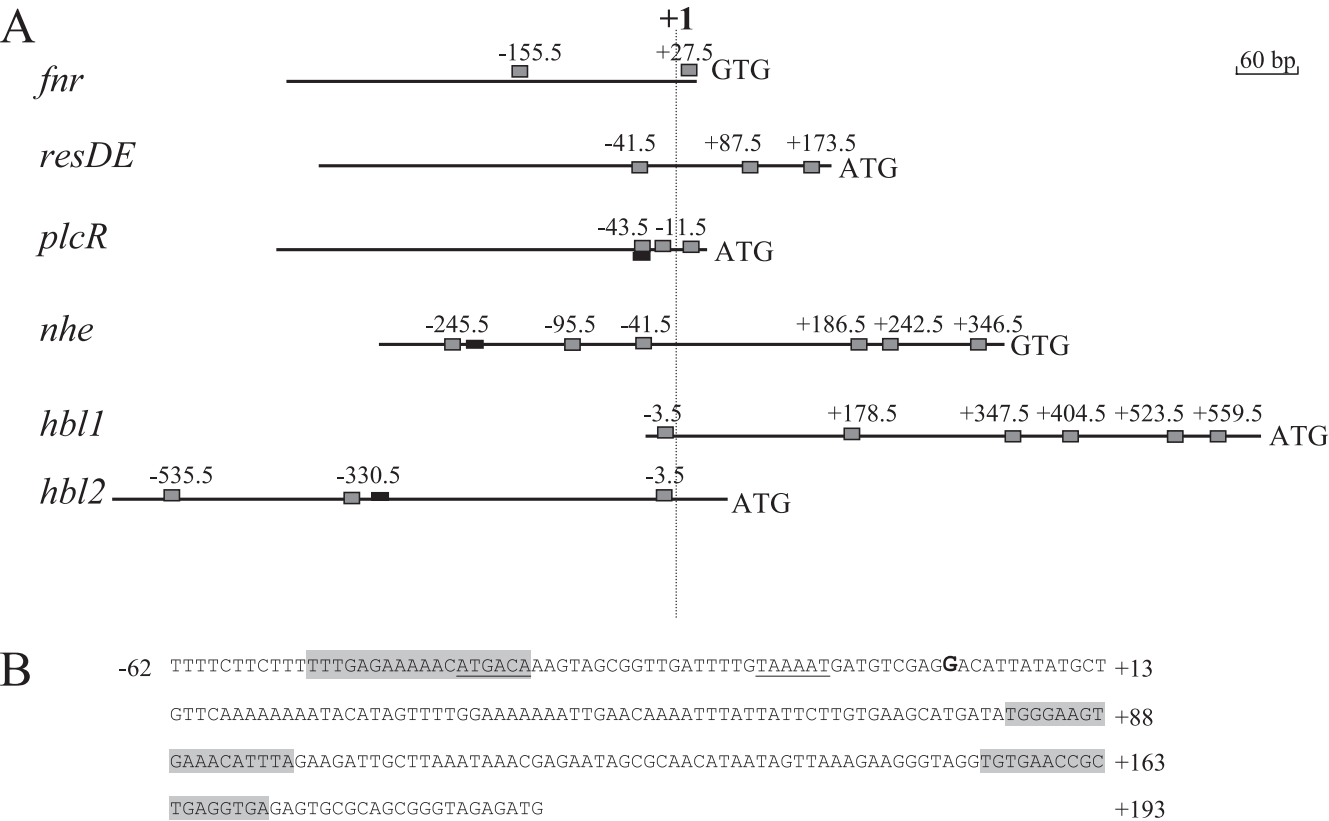


FIG. 4. Potential Fnr-binding sites in the 5' untranslated regions of *fnr*, *resDE*, *plcR*, *hbl*, and *nhe*. All numbering is relative to the transcription start site at position +1. (A) Potential Fnr-binding sites are shown relative to the transcription start site as gray boxes. PlcR boxes are shown as black boxes. (B) Genetic organization of the *resDE* promoter region. The transcriptional start site (+1) determined by 5' RACE PCR is in bold type. The putative -35 and -10 motifs are underlined. Putative Crp/Fnr boxes are indicated by a gray background.

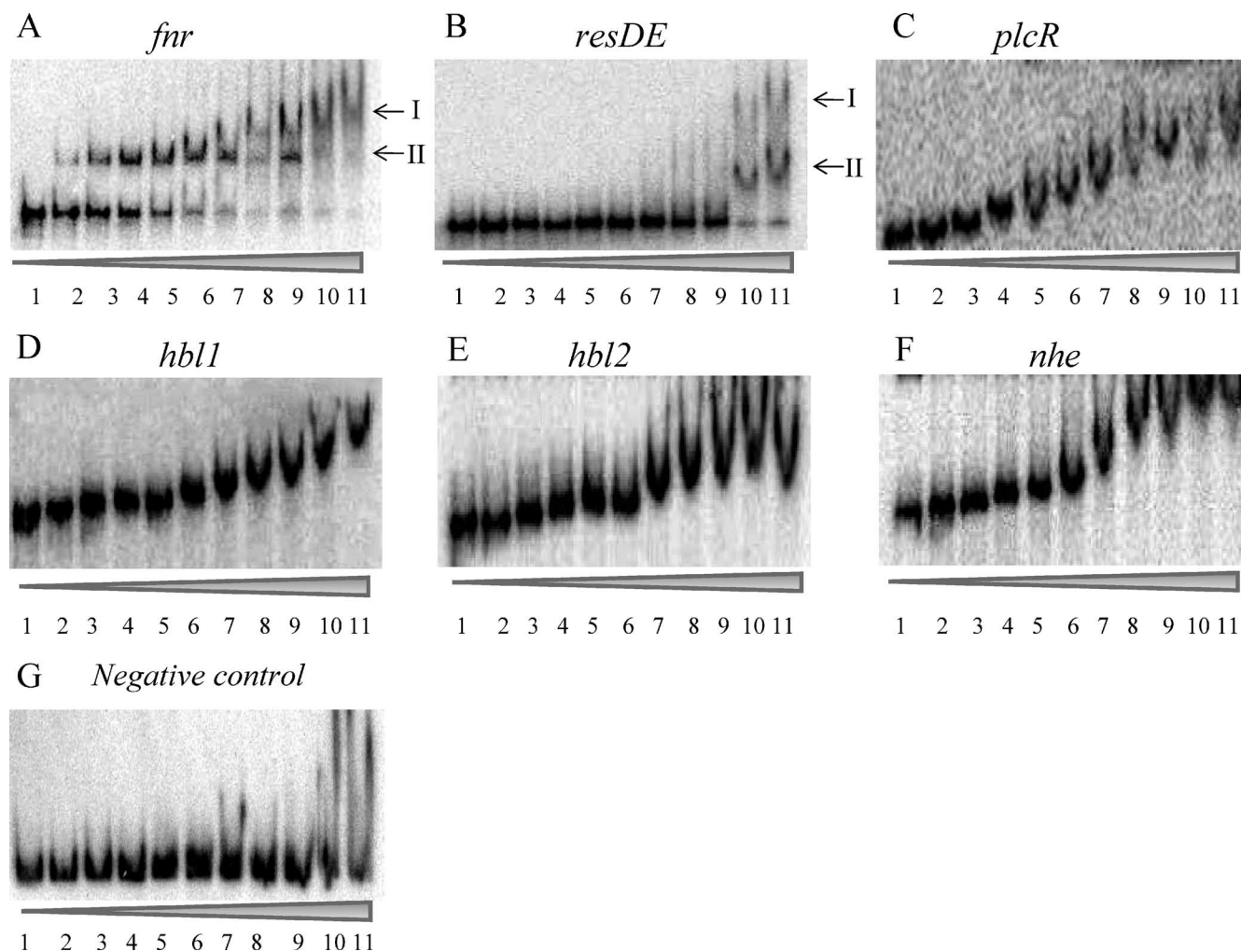


FIG. 5. Binding of apoFnr to 5'UTRs of *fnr*, *resDE*, *plcR*, *hbl*, and *nhe* genes determined by EMSAs. DNAs corresponding to *fnr* (A), *resDE* (B), *plcR* (C), *hbl1* (D), *hbl2* (E), *nhe* (F), and a negative control (G) were bound with increasing concentrations of apoFnr as indicated by the height of the triangle below the gel. The results presented are representative examples of an experiment performed in triplicate with either purified Fnr_{His} or with reduced Strep_{Fnr} (purified Strep_{Fnr} plus 200 mM DTT). Lanes 1 to 11 contain 0, 0.2, 0.4, 0.6, 0.8, 1, 2, 3, 4, 5, and 6 μ M apoFnr protein, respectively.

as more protein was added, the protein complex bound to the DNA increased proportionally in size, with the added apoFnr being distributed evenly among all the complexes. The smearing of these species during EMSA also suggested that these high-molecular-weight complexes were not stable and dissociated during electrophoresis. The EMSA data also showed that the *plcR*, *hbl*, and *nhe* 5'UTRs were bound by apoFnr with a lower affinity (equilibrium dissociation constant [K_D] of ≤ 0.4 μ M) than the *resDE* and *fnr* promoter regions (K_D s of 3 and 4.5 μ M, respectively).

To test whether the oligomeric state regulated the DNA-binding activity of both Fnr_{His} and Strep_{Fnr}, the effect of the reducing agent DTT (200 mM) on the binding of Strep_{Fnr} and the effect of the oxidizing agent diamide (1 mM) on the binding of Fnr_{His} to all promoter regions were investigated. Adding reductant resulted in the generation of Strep_{Fnr}-DNA complex patterns similar to those obtained with Fnr_{His} (Fig. 5). The effect of DTT was reversible, while the addition of diamide (1 mM) abolished Strep_{Fnr} binding (data not shown). Likewise,

Fnr_{His} showed no DNA-binding activity in the presence of diamide (data not shown). Thus, the oligomeric state of apoFnr was found to critically affect its binding activity. The data also indicate that apoFnr was able to bind the *fnr*, *resDE*, *plcR*, *hbl*, and *nhe* 5'UTRs only when present predominantly as a monomer.

DISCUSSION

Our previous studies showed that aerobic enterotoxin expression was regulated by both the transcriptional regulator Fnr and oxygen availability (or redox state) under aerobiosis (4, 33). In the present work, we describe experimental evidence for redox regulation of enterotoxin gene expression mediated by Fnr through its DNA-binding properties.

B. cereus apoFnr was overexpressed in *E. coli* and purified as either a C-terminal His-tagged (Fnr_{His}) or an N-terminal Strep-tagged (Strep_{Fnr}) fusion protein. Unlike Fnr_{His}, Strep_{Fnr} was purified without an affinity chromatography step. The rea-

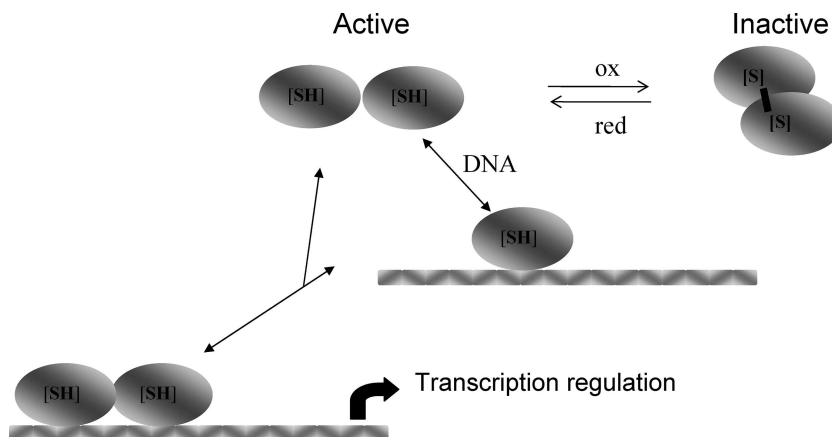


FIG. 6. Proposal for the regulation of apoFnr activity by a thiol-disulfide redox switch. Brackets indicate that one or more disulfide bonds may be involved.

son was the poor affinity of the *Strep*-tag peptide (IBA BioTAGnology) for streptavidin (Strep-Tactin) due to its fusion to the N terminus of Fnr (19). No such problem was encountered in the case of Strep-tagged *B. subtilis* Fnr (27). This different behavior may be explained by the marked difference in the two N-terminal polypeptide sequences. Both recombinant Fnr (Fnr_{His} and *Strep*-Fnr) were produced in multiple oligomeric apoforms. The distribution of quaternary structures was shown to differ between the two tagged variants. Purified Fnr_{His} was predominantly monomeric, while *Strep*-Fnr was predominantly oligomeric, and the oligomerization of *Strep*-Fnr appeared to be due to the formation of disulfide bridges. Data obtained from crystal structure analysis of a member of the Crp/Fnr family showed that dimerization involved the C-terminal domain (13). This suggests that extension of *B. cereus* Fnr at its C terminus may introduce steric hindrance that reduces flexibility and/or affects interdomain communication. In turn, this would result in a less permissive, locked conformation, rendering the thiol group less exposed for pairing to form the disulfide bond.

Our results showed that the active DNA-binding form of both recombinant apoFnrs was the monomer. Diamide treatment inactivated monomeric apoFnr in a DTT-reversible manner, suggesting that it was subject to redox regulation. In addition, we detected the presence of disulfide-linked endogenous dimers in *B. cereus* cells. Taken together, these findings suggest that formation of stabilized dimeric apoFnr by means of one or more SS bonds may be a regulatory mechanism that controls Fnr binding under exposure to oxidizing conditions. Figure 6 shows the scheme we propose for the reversible activation/inactivation of *B. cereus* apoFnr. It implies that this protein mediates a response to oxygen concentration and/or redox state causing the repression or activation of relevant genes. Such a thiol-based redox switch has been observed with *Desulfitobacterium dehalogenans* CrpK, a member of the Crp/Fnr family (24, 25). In this bacterium, the redox switch involves formation of an intermolecular disulfide bond that links two CprK subunits in an inactive dimer. Although it belongs to the same family, *B. cereus* Fnr contains three more cysteines than CprK does and should have the capacity to bind a FeS cluster like *B. subtilis* Fnr (27). For this reason, our findings are original. Additional work is now required to determine which of

the seven cysteine residues are involved in this redox state sensing.

Many transcription factors bind DNA to form dimeric protein-DNA complexes. For these proteins, there are two limiting pathways that can describe the route of complex assembly. The protein can dimerize first and then associate with DNA (dimer pathway), or it can follow a pathway in which two monomers bind DNA sequentially and assemble their dimerization interface while bound to DNA (monomer pathway) (15). Many regulators bind DNA by the dimer pathway, and this is the case for Fnr of *B. subtilis* and *E. coli* under anaerobiosis (27). Under aerobiosis, apoFnr is produced as an inactive monomer in *E. coli* (28) and as an inactive dimer in *B. subtilis* (27). Because only the monomeric form of *B. cereus* apoFnr binds to DNA, we propose that Fnr binding in *B. cereus* occurs via the monomer pathway under aerobiosis (Fig. 6). Binding through the monomer pathway allows a dimeric transcription factor to respond rapidly to stimuli and to locate its target site quickly without becoming entrapped kinetically at a nonspecific site (23). Therefore, in addition to a faster assembly of apoFnr-DNA complexes in response to oxygen tension in the environment allowed by the monomer pathway, an efficient way to discriminate between specific and nonspecific target sites is also provided.

Since apoFnr bound to the promoter regions of *fnr* itself, the two-component system *resDE* genes, the virulence regulator *plcR* gene, and the enterotoxin genes *hbl* and *nhe*, we concluded that apoFnr directly controlled both its own expression and that of *resDE*, *plcR*, *hbl*, and *nhe* (34). The relatively low DNA-binding affinity observed for apoFnr suggests that other factors may be involved in DNA recognition as well as in protein-DNA complex stabilization (16). For example, it is conceivable that apoFnr operates with a specific oxidoreductase system or that for some other reason the cytoplasmic environment provided by *B. cereus* enhances its site-specific DNA-binding ability. In addition, interaction of apoFnr with one or more other regulatory proteins may facilitate its interaction with DNA. High-affinity binding to 5'UTRs of enterotoxin genes may require apoFnr-PlcR interaction insofar as PlcR (1) possesses binding sites close to the predicted Fnr-

binding sites (Fig. 4A). Another possible interaction partner of apoFnr is the redox regulator ResD (4).

Transcriptional regulators such as members of the Crp/Fnr family interact with the α subunit of RNA polymerase (RNAP) (10). It has been shown that the protein-protein interaction increases the affinity of both partners to the promoter site (2). The contacts established between a Crp/Fnr protein and RNAP involve three patches of surface-exposed amino acids (called activating regions 1, 2, and 3) of Crp/Fnr protein. These contacts depend on the specific architecture of each promoter. The Crp/Fnr-dependent promoters can be grouped into three classes (labeled I, II, and III) based on the number and position of the Crp/Fnr-binding sites relative to the start of transcription and on the mechanism for transcription activation (2). The upstream DNA-binding site in class I promoters is centered either at position -61.5 (i.e., its axis of symmetry is between positions -61 and -62) or one to three helical turns further upstream (i.e., -71.5 , -82.5 , or -92.5). In class II promoters, the symmetry axis of the binding site is located at position -41.5 relative to the transcription start site, thus overlapping with the -35 region. Class III promoters comprise two or more DNA-binding sites for Crp/Fnr and have various architectures according to both the spacing between the DNA-binding sites and the distance between the Crp/Fnr-DNA-binding sites and RNAP-DNA-binding sites. In the case of *B. cereus*, the locations of predicted Crp/Fnr-binding sites upstream of the transcriptional start site suggest that the *B. cereus* *fnr* promoter region is a class I activating promoter, while *resDE* and *plcR* promoter regions are class II promoters. The *nhe* and *hbl* promoters are different and may be considered class III Crp/Fnr-dependent activated promoters. However, *nhe*, *hbl*, and to a lesser extent *fnr*, *resDE*, and *plcR* promoter regions, also contain predicted Crp/Fnr boxes located close to the -10 region and/or downstream of the transcriptional start site, i.e., at positions different from those found in classical Crp/Fnr-activated promoters. Comparable results were found for *E. coli* and *B. subtilis* Fnr (9, 27), where repression of transcription is mediated by Fnr binding to sites in different locations than in activating sites. Thus, we hypothesize that the regulation of enterotoxin gene expression involves an interplay of transcriptional activation and repression by Fnr. Repression may be mediated by occupancy of sites located downstream of the $+1$ site. In conclusion, the mechanism of Fnr-dependent regulation of enterotoxin in *B. cereus* is undoubtedly complex, and further extensive studies are required to examine the essential role of the downstream binding sites. Importantly, both *hbl* and *nhe* promoters have a long UTR (Fig. 4A), making it likely that mechanisms at the posttranscriptional level also control their expression. Such regulation could involve interaction between transcriptional regulators and ribosomal proteins (8). Finally, deciphering the complexities of this Fnr-dependent regulation is necessary to fully understand the mechanisms employed by *B. cereus* to ensure optimal virulence gene expression in response to changes in oxygen tension such as those encountered during infection in a human host.

In conclusion, this work shows that unlike its homologue in *B. subtilis* (12, 27), *B. cereus* Fnr is able to function as a transcriptional factor independently of the integrity of the FeS cluster. Thus, *B. cereus* Fnr illustrates the great versatility of the archetypal Crp/Fnr structure for transducing environmen-

tal signals to the transcriptional apparatus. More importantly, this study expands our knowledge of the molecular mechanisms used in *B. cereus* to modulate the transcriptional level of enterotoxin genes in response to redox variations.

ACKNOWLEDGMENTS

J.E. held a fellowship from the Ministère de la Recherche et de l'Enseignement Supérieur.

We thank Christine Meyer (CEA-Grenoble) for her help and technical advice in protein purification, Bernard Fernandez (CEA-Marcoule) for conducting DLS experiments, Jean-Charles Gaillard (CEA-Marcoule) for mass spectrometry measurements, and Valérie Tanchou (CEA-Marcoule) for her kind help in the production of polyclonal antibodies.

REFERENCES

- Agaisse, H., M. Gominet, O. A. Okstad, A. B. Kolsto, and D. Lereclus. 1999. PlcR is a pleiotropic regulator of extracellular virulence factor gene expression in *Bacillus thuringiensis*. *Mol. Microbiol.* **32**:1043–1053.
- Busby, S., and R. H. Ebright. 1999. Transcription activation by catabolite activator protein (CAP). *J. Mol. Biol.* **293**:199–213.
- Duport, C., S. Thomassin, G. Bourel, and P. Schmitt. 2004. Anaerobiosis and low specific growth rates enhance hemolysin BL production by *Bacillus cereus* F4430/73. *Arch. Microbiol.* **182**:90–95.
- Duport, C., A. Zigha, E. Rosenfeld, and P. Schmitt. 2006. Control of enterotoxin gene expression in *Bacillus cereus* F4430/73 involves the redox-sensitive ResDE signal transduction system. *J. Bacteriol.* **188**:6640–6651.
- Folta-Stogniew, E. 2006. Oligomeric states of proteins determined by size-exclusion chromatography coupled with light scattering, absorbance, and refractive index detectors. *Methods Mol. Biol.* **328**:97–112.
- Gabant, G., J. Augier, and J. Armengaud. 2008. Assessment of solvent residues accessibility using three Sulfo-NHS-biotin reagents in parallel: application to footprint changes of a methyltransferase upon binding its substrate. *J. Mass Spectrom.* **43**:360–370.
- Gohar, M., O. A. Okstad, N. Gilois, V. Sanchis, A. B. Kolsto, and D. Lereclus. 2002. Two-dimensional electrophoresis analysis of the extracellular proteome of *Bacillus cereus* reveals the importance of the PlcR regulon. *Proteomics* **2**:784–791.
- Gray, J. P., J. W. Davis II, L. Gopinathan, T. L. Leas, C. A. Nugent, and J. P. Vanden Heuvel. 2006. The ribosomal protein rplL1 associates with and inhibits the transcriptional activity of peroxisome proliferator-activated receptor- α . *Toxicol. Sci.* **89**:535–546.
- Green, J., A. S. Irvine, W. Meng, and J. R. Guest. 1996. FNR-DNA interactions at natural and semi-synthetic promoters. *Mol. Microbiol.* **19**:125–137.
- Green, J., C. Scott, and J. R. Guest. 2001. Functional versatility in the CRP-FNR superfamily of transcription factors: FNR and FLP. *Adv. Microb. Physiol.* **44**:1–34.
- Guinebretiere, M. H., and C. Nguyen-The. 2003. Sources of *Bacillus cereus* contamination in a pasteurized zucchini purée processing line, differentiated by two PCR-based methods. *FEMS Microbiol. Ecol.* **43**:207–215.
- Guinebretiere, M. H., F. L. Thompson, A. Sorokin, P. Normand, P. Dawyndt, M. Ehling-Schulz, B. Svensson, V. Sanchis, C. Nguyen-The, M. Heyndrickx, and P. De Vos. 2008. Ecological diversification in the *Bacillus cereus* group. *Environ. Microbiol.* **10**:851–865.
- Joyce, M. G., C. Levy, K. Gabor, S. M. Pop, B. D. Biehl, T. I. Doukov, J. M. Ryter, H. Mazon, H. Smidt, R. H. van den Heuvel, S. W. Ragsdale, J. van der Oost, and D. Leys. 2006. CprK crystal structures reveal mechanism for transcriptional control of halorespiration. *J. Biol. Chem.* **281**:28318–28325.
- Khoroshilova, N., H. Beinert, and P. J. Kiley. 1995. Association of a polynuclear iron-sulfur center with a mutant FNR protein enhances DNA binding. *Proc. Natl. Acad. Sci. USA* **92**:2499–2503.
- Kohler, J. J., S. J. Metallo, T. L. Schneider, and A. Schepartz. 1999. DNA specificity enhanced by sequential binding of protein monomers. *Proc. Natl. Acad. Sci. USA* **96**:11735–11739.
- Korner, H., H. J. Sofia, and W. G. Zumft. 2003. Phylogeny of the bacterial superfamily of Crp-Fnr transcription regulators: exploiting the metabolic spectrum by controlling alternative gene programs. *FEMS Microbiol. Rev.* **27**:559–592.
- Kotiranta, A., K. Lounatmaa, and M. Haapasalo. 2000. Epidemiology and pathogenesis of *Bacillus cereus* infections. *Microbes Infect.* **2**:189–198.
- Laemmli, U. K. 1970. Cleavage of structural proteins during the assembly of the head of bacteriophage T4. *Nature* **227**:680–685.
- Maier, T., N. Drapal, M. Thanbichler, and A. Bock. 1998. Strep-tag II affinity purification: an approach to study intermediates of metalloenzyme biosynthesis. *Anal. Biochem.* **259**:68–73.
- Okstad, O. A., M. Gominet, B. Purnelle, M. Rose, D. Lereclus, and A. B. Kolsto. 1999. Sequence analysis of three *Bacillus cereus* loci carrying PlcR-regulated genes encoding degradative enzymes and enterotoxin. *Microbiol. og* **145**:3129–3138.

21. **Ouhib, O., T. Clavel, and P. Schmitt.** 2006. The production of *Bacillus cereus* enterotoxins is influenced by carbohydrate and growth rate. *Curr. Microbiol.* **53**:222–226.
22. **Pelley, J. W., C. W. Garner, and G. H. Little.** 1978. A simple rapid biuret method for the estimation of protein in samples containing thiols. *Anal. Biochem.* **86**:341–343.
23. **Pomerantz, J. L., S. A. Wolfe, and C. O. Pabo.** 1998. Structure-based design of a dimeric zinc finger protein. *Biochemistry* **37**:965–970.
24. **Pop, S. M., N. Gupta, A. S. Raza, and S. W. Ragsdale.** 2006. Transcriptional activation of dehalorespiration. Identification of redox-active cysteines regulating dimerization and DNA binding. *J. Biol. Chem.* **281**:26382–26390.
25. **Pop, S. M., R. J. Kolarik, and S. W. Ragsdale.** 2004. Regulation of anaerobic dehalorespiration by the transcriptional activator CprK. *J. Biol. Chem.* **279**:49910–49918.
26. **Ramarao, N., and D. Lereclus.** 2006. Adhesion and cytotoxicity of *Bacillus cereus* and *Bacillus thuringiensis* to epithelial cells are FlhA and PlcR dependent, respectively. *Microbes Infect.* **8**:1483–1491.
27. **Reents, H., I. Gruner, U. Harmening, L. H. Bottger, G. Layer, P. Heathcote, A. X. Trautwein, D. Jahn, and E. Hartig.** 2006. *Bacillus subtilis* Fnr senses oxygen via a [4Fe-4S] cluster coordinated by three cysteine residues without change in the oligomeric state. *Mol. Microbiol.* **60**:1432–1445.
28. **Reinhart, F., S. Achebach, T. Koch, and G. Uden.** 2008. Reduced apo-fumarate nitrate reductase regulator (apoFNR) as the major form of FNR in aerobically growing *Escherichia coli*. *J. Bacteriol.* **190**:879–886.
29. **Rosenfeld, E., C. Duport, A. Zigha, and P. Schmitt.** 2005. Characterisation of aerobic and anaerobic vegetative growth of the food-borne pathogen *Bacillus cereus*. *J. Can. Microbiol.* **51**:149–158.
30. **Schoeni, J. L., and A. C. Wong.** 2005. *Bacillus cereus* food poisoning and its toxins. *J. Food Prot.* **68**:636–648.
31. **Slamti, L., and D. Lereclus.** 2002. A cell-cell signaling peptide activates the PlcR virulence regulon in bacteria of the *Bacillus cereus* group. *EMBO J.* **21**:4550–4559.
32. **Spira, W. M., and J. M. Goepfert.** 1975. Biological characteristics of an enterotoxin produced by *Bacillus cereus*. *Can. J. Microbiol.* **21**:1236–1246.
33. **Zigha, A., E. Rosenfeld, P. Schmitt, and C. Duport.** 2006. Anaerobic cells of *Bacillus cereus* F4430/73 respond to low oxidoreduction potential by metabolic readjustments and activation of enterotoxin expression. *Arch. Microbiol.* **185**:222–233.
34. **Zigha, A., E. Rosenfeld, P. Schmitt, and C. Duport.** 2007. The redox regulator Fnr is required for fermentative growth and enterotoxin synthesis in *Bacillus cereus* F4430/73. *J. Bacteriol.* **189**:2813–2824.